Table 1. Characteristics of the Patients

	Total	Idiopathic	Congenital	Symptomatic
No. patients (male:female)	32 (8:24)	18 (3:15)	8 (3:5)	6 (2:4)
Age at the latest follow-up (yrs)	36.4 (30.6–43.8)	36.4	36.8	35.7
Duration of follow-up (yrs)	21.1 (16.5–28.9)	20.6	23.1	19.9
Age at time of surgery (yrs)	15.3 (10.9–22.2)	15.9	13.7	15.8
Type of surgery	Harrington: 14 Cotrel-Dubousset: 11 Zielke: 4 Dywer: 2 C-D and Zielke: 1	Harrington: 7 Cotrel-Dubousset: 8 Zielke: 2 Dywer: 1	Harrington: 7 Dywer: 1	Cotrel-Dubousset: 3 Zielke: 2 C-D and Zielke: 1

the incidence and severity of LBP. In addition, the patients were asked to complete a questionnaire to evaluate long-term outcome. The evaluation was performed by the first author (K.T.), who was unbiased and not involved in the primary care of the patients.

Physical Examination

Present height and weight were measured and Body Mass Index was calculated. Rib and lumbar humps were measured with a scoliometer. Spinal balance was evaluated with a plumb line from the C7 spinous process to the intergluteal crease, and leg length discrepancy was assessed in millimeters.

Radiologic Evaluation

Standing posteroanterior and lateral plain radiograph examinations of the whole spine were performed. Radiologic evaluation included preoperative Cobb angle, correction ratio with surgical treatment, loss of correction of Cobb angle at the latest follow-up, lumbar lordosis measured between cranial L1 endplate and caudal L5 endplate, and sagittal balance, defined as anterior deviation of a line drawn perpendicularly from the center of the C7 vertebral body to the posterocranial corner of the sacrum.[20] In addition, degenerative changes of the subjacent segment were evaluated using the modified Weiner grading system,[21] based on disc space narrowing (at least 25%), spur formation, eburnation, and listhesis.

Contents of Interview

Patients were interviewed regarding LBP. Degree of LBP was evaluated by visual analogue scale (VAS) score (range, 0–100) and also by Moskowitz classification.[2] The severity of LBP was graded from I to V: Grade I indicates no pain; Grade II indicates rare pain, with patients not admitting to pain unless pressed to do so, and pain usually brought about by strenuous activity; Grade III indicates occasional pain, experienced a few times each year, with the patient admitting to pain without questioning, which is never severe enough to require a visit to a physician and is brought on by increased activity or prolonged sitting; Grade IV indicates frequent pain, after activity but not restrictive, requiring pain medication or muscle relaxants and visits to a physician; and Grade V indicates constant pain, (*a*) not incapacitating or (*b*) incapacitating. Patients classified as Grade I or Grade II were considered able to perform daily activities without LBP.

The official Japanese version of the SF-36 was used to evaluate both the physical and mental status of the patients. The SF-36 consists of 36 questions on the general health status of patients, and scores for 8 specific physical and emotional categories were obtained.

Statistical Analysis

Values are the mean ± SD for each group. The significance of differences in parameters between groups was tested using one-way analysis of variance, with *post hoc* testing performed using the Scheffe method. *P* values less than 0.05 were considered significant.

■ Results

Clinical Examination

Mean height was 154.4 cm (range, 106–174.3), mean weight 49.3 kg (range, 27–66.9), and mean Body Mass

Table 2. Clinical Examination

	Total	Idiopathic	Congenital	Symptomatic
Height (cm)	154.4 (106–174.3)	157.6	155.8	142.9
Weight (kg)	49.3 (27–66.9)	48.9	51.3	48.0
Body mass index (kg/m^2)	20.5 (15.3–32.1)	19.6	21.2	22.5
Rib hump (mm)	19.2 (0–75)	23.8	13.8	12.5
Lumbar hump (mm)	2.8 (0–35)	3.1	3.1	1.7
Plumb line (mm)	11.0 (0–50)	9.1	7.5	21.7
Leg length discrepancy (mm)	8.9 (0–20)	7.5	6.3	18.0

Table 3. Radiological Evaluation

	Total	Idiopathic	Congenital	Symptomatic
Preoperative cobb angle (°)	69.8 (32–140)	65.1	54.5	104.7
Postoperative cobb angle (°)	33.0 (4–95)	30.9	30.5	49.8
Rates of operative correction (%)	53.7 (18.1–107.1)	57.1	46.0	53.5
Cobb angle at the latest follow-up (°)	41.7 (11–106)	39.5	36.8	60.0
Loss of correction (°)	8.7 (0–42)	8.6	6.3	11.2
Lumbar lordosis (°)	31.7 (7–53)	33.8	31.9	23.8
Positive sagittal balance (mm)	19/32 (21.7)	8/18 (7.9)	6/8 (27.6)	5/6 (62.0)
Degenerative change of subjacent segment	6/32	5/18	0/8	1/6
No. levels of fusion (vertebrae)	9.1 (2–15)	9.8	7.1	9.5

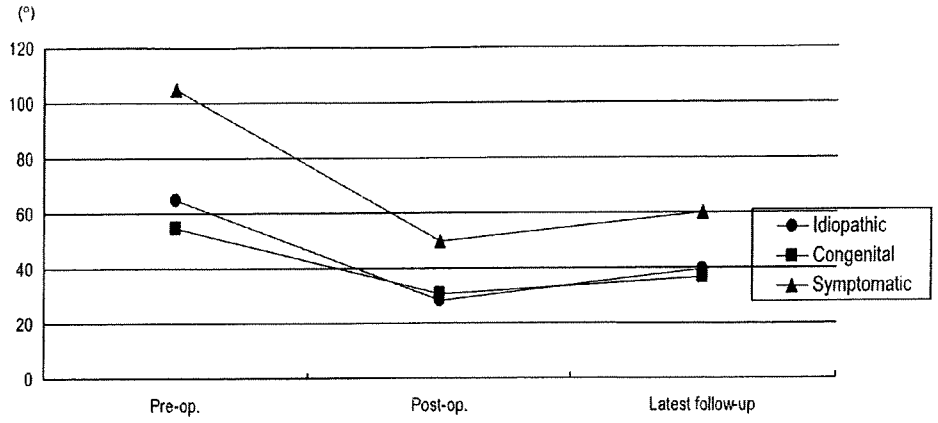

Figure 1. Change in Cobb angle by type of scoliosis. Patients with symptomatic scoliosis had a significantly higher preoperative Cobb angle, though no significant differences were found among the groups in postoperative Cobb angle, ratio of operative correction, Cobb angle at the latest follow-up, or degree of loss of correction.

Index 20.5 kg/m^2 (range, 15.3–32.1) at the latest follow-up (Table 2). The mean degree of rib hump was 19.2 mm (range, 0–75), and the mean degree of lumbar hump 2.8 mm (range, 0–35).

Radiologic Evaluation

Cobb angle improved from a mean of 69.8° (range, 32–140) before surgery to 33° (range, 4–95) after surgery (Table 3, Figure 1). The mean ratio of operative correction was 53.7% (range, 18.1–107.1). The mean Cobb angle at the latest follow-up was 41.7° (range, 11–106), with a mean of 8.7° (range, 0–42) in loss of correction over 16-year follow-up. By type of scoliosis, patients with symptomatic scoliosis had a significantly higher preoperative Cobb angle, but no significant differences were observed among the groups in postoperative Cobb angle, ratio of operative correction, Cobb angle at the latest follow-up, or degree of loss of correction.

By type of instrumentation, the mean ratio of operative correction was 50.4% with Harrington instrumentation, 53.1% with C-D, 72.5% with Zielke, 42.1% with Dywer, and 53.4% with C-D with Zielke. Mean loss of correction was 6.9° with Harrington instrumentation, 6.6° with C-D, 20.3° with Zielke, 5.5° with Dywer, and 9.0° with C-D with Zielke.

Mean lumbar lordosis was 31.7° (range, 7–53), 19 patients (59.4%) had positive sagittal balance, and the mean degree of deviation was 21.7 mm (range, −45 to 140). Six patients (18.8%) had degenerative changes of the subjacent segment. The mean number of levels of fusion was 9.1 vertebrae (range, 2–15).

Table 4. VAS Score and Moskowitz Classification

	Total	Idiopathic	Congenital	Symptomatic
VAS score (0–100)	21.4	18.1	32.9	16.0
Moskowitz classification (no. patients)				
Grade I; no pain	14	8	1	5
Grade II; rare pain	13	9	4	0
Grade III; occasional pain	2	0	2	0
Grade IV; frequent pain	3	1	1	1
Grade V; constant pain	0	0	0	0

Revision Surgery

Five patients underwent surgery for removal of instrumentation while asymptomatic, and 3 underwent revision surgery due to instrument failure within 2 years after surgery for scoliosis.

VAS Score

The mean VAS score at the latest follow-up was 21.4 (range, 0–80). There were no significant differences in score among types of scoliosis (Table 4).

Moskowitz Classification

Fourteen patients (43.8%) had no pain, 13 patients (40.6%) had rare pain, 2 patients (6.3%) occasional pain, 3 patients (9.4%) frequent pain, and no patient had constant pain (Table 4).

SF-36 Questionnaire

The score for bodily pain did not differ from that for age-matched controls (Table 5). In the case of symptomatic scoliosis, scores for physical function, role-physical, social function, and role-emotional were significantly low. However, none of the scores for subjects with idiopathic or congenital scoliosis were markedly different from those for age-matched healthy controls.

Correlations Between Radiologic Findings and Degree of LBP

Level of distal fusion had no effect on the incidence or severity of LBP as evaluated by Moskowitz classification

Table 5. SF-36 Norm-Based Scoring Scores

	Total	Idiopathic	Congenital	Symptomatic
Physical function	46.0 ± 17.1	53.0	49.4	20.5*
Role-physical	48.4 ± 12.6	50.8	51.1	37.5*
Bodily pain	50.1 ± 9.9	50.6	47.8	51.5
General health	48.1 ± 10.5	47.7	49.1	47.9
Vitality	48.3 ± 10.5	48.4	47.6	49.2
Social function	52.8 ± 7.9	53.4	57.1	45.0*
Role-emotional	50.3 ± 10.4	51.4	55.0	41.0*
Mental health	51.7 ± 7.2	51.3	51.8	52.7

*$P < 0.05$

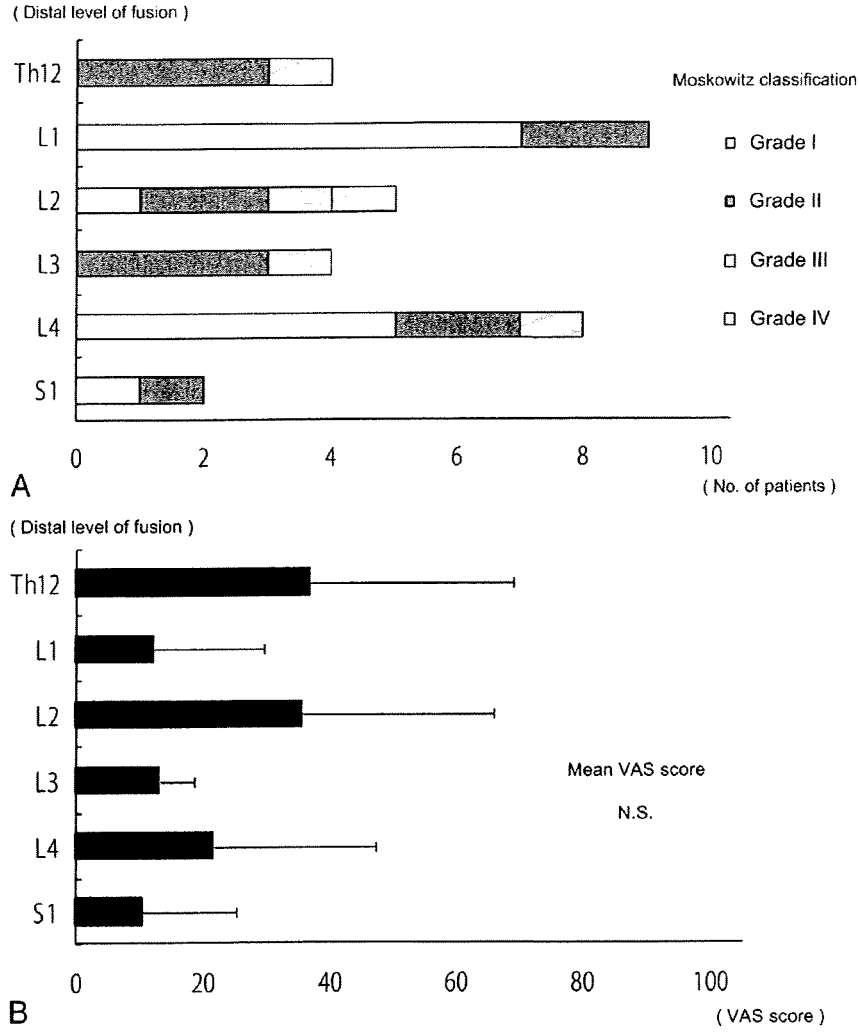

Figure 2. Correlations between distal level of fusion and Moskowitz classification (**A**) and VAS score (**B**). There were no differences in Moskowitz classification among distal levels of fusion, and no significant differences in VAS score were found among such levels.

and VAS score (Figure 2A, 2B). Furthermore, preoperative Cobb angle, latest Cobb angle, and degenerative changes of the subjacent segment each exhibited no correlation with degree of LBP, either (Figures 3–5). On the other hand, sagittal balance at the latest follow-up affected LBP, with patients with positive sagittal balance exhibiting significant LBP (Figure 6).

■ Discussion

Correction of spinal deformity with instrumentation is an established procedure in scoliosis surgery, and good clinical outcomes have been reported with it even on long-term evaluation.[7,8,14–18,22,23]

However, measures of long-term outcome in scoliosis surgery have mainly focused on radiologic changes such as correction ratio of Cobb angle and loss of correction. Recently published studies suggest that these parameters are only weakly related to functional status,[1] while subjective symptoms such as LBP after surgical treatment are of great concern to patients with scoliosis. LBP is especially important in long-term follow-up studies, which can yield reliable findings for patients who will undergo scoliosis surgery. The incidence of LBP after surgery for scoliosis have been quite wide-ranging (from 7% to 66%) in previous studies.[2–19]

Many studies have reported various factors contributing to LBP (*e.g.*, distal level of fusion, preoperative Cobb angle, latest Cobb angle, and lack of correlation with radiologic findings, among others).[10–19] Padua *et al* reported long-term outcomes in AIS patients after Harrington instrumentation.[15] They found that patients functioned well socially, and that only 9.4% of them had LBP. They also found significant correlation between LBP impairment and preoperative Cobb angle.

Danielsson and Nachemson reported long-term outcomes regarding back pain and function in a large series of patients treated for AIS involving comparison with matched control subjects who did not have scoliosis.[19] They found that LBP, though mild (average VAS score 24), was significantly more frequent among the patients than the controls (65% *vs.* 47%), but that this had little effect on daily life and function. They also found that the patients had significantly more degenerative disc change than the controls, although no cor-

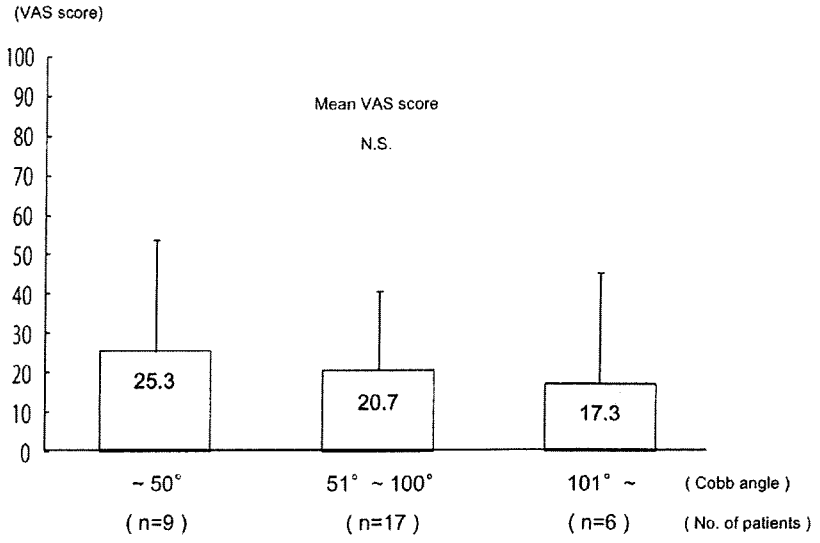

Figure 3. Correlation between preoperative Cobb angle and VAS score. No correlation was found.

relations could be found between LBP and various radiologic variables.

Weinstein *et al* reported long-term outcomes related to health and function in untreated patients with AIS, by comparison with matched controls.[24] They found that untreated adults with AIS exhibited a high level of function at 50-year follow-up, and that patients had little physical impairment other than LBP.

There have recently been some reports of LBP in adult patients with scoliosis including those with AIS and *de novo* degenerative scoliosis.[25–27] Schwab *et al*, reporting clinical and radiologic findings for adult patients with scoliosis,[25] found that patients with AIS had more pronounced scoliotic curvature than patients with *de novo* degenerative scoliosis. In their study, mean VAS score was 58, and lateral vertebral olisthy, L3 and L4 endplate obliquity angles, lumbar lordosis, and thoracolumbar kyphosis were significantly correlated with LBP.

The SF-36 is the instrument most widely used for evaluation of QOL in adults patients.[28] It consists of 8 subscales including physical function, role-physical, bodily pain, general health, vitality, social functioning, role-emotional, and mental health. Although it includes neither a score for self-image nor a factor unique to patients with scoliosis,[29] we used it for comparison with age-matched controls.

In the present study, the score for bodily pain in patients did not differ from that for controls. In the case of symptomatic scoliosis, scores for physical function, role-physical, social function, and role-emotional were significantly low. However, none of the scores for subjects with idiopathic or congenital scoliosis were markedly different from those for age-matched healthy controls.

In the present study, mean VAS score at the latest follow-up was 21.4, and 5 patients (15.6%) had occasional and frequent LBP. Incidences of LBP are hard to

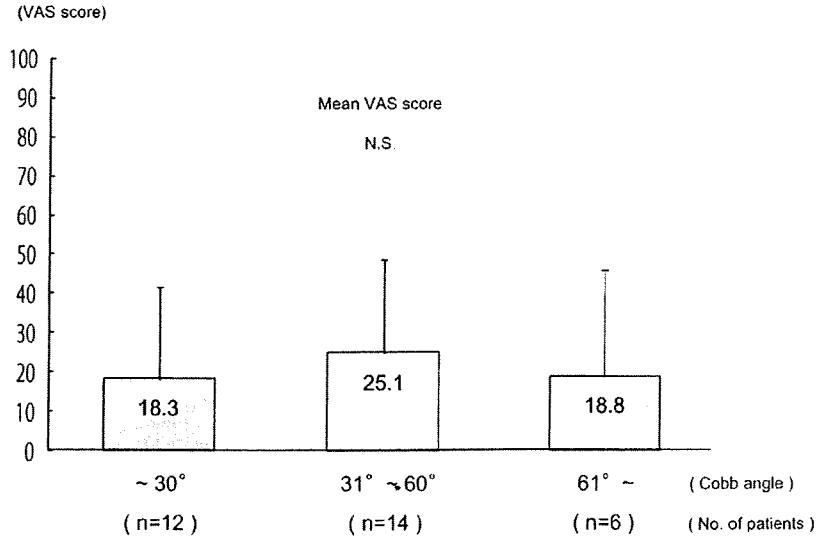

Figure 4. Correlation between latest Cobb angle and VAS score. No correlation was found.

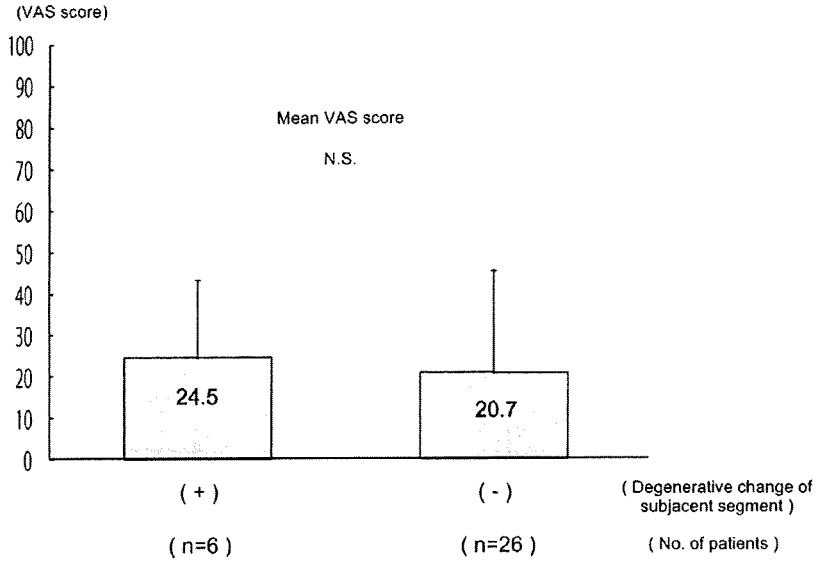

Figure 5. Correlation between degenerative change of subjacent segment and VAS score. Although 6 patients (18.8%) had degenerative changes of the subjacent segment, their mean VAS score was not significantly different from that of the other patients.

compare, since it is difficult to determine standards for subjective complaints such as LBP. We therefore evaluated patients using the Moskowitz classification.[2] The rate of LBP in our patients is similar to those in previous studies, and no more frequent than that in the normal population in Japan (2004, Japan, Comprehensive Survey of Living Condition of the People on Health and Welfare).

We found that distal level of fusion, preoperative Cobb angle, latest Cobb angle, and degenerative changes of the subjacent segment each exhibited no correlation with the degree of LBP, but did find that positive sagittal balance at the latest follow-up affected degree of LBP.

Glassman *et al* examined 752 patients with adult deformity, and found that severity of symptoms increased linearly with degree of progression of positive sagittal balance.[20] These findings emphasize the importance of carefully ensuring sagittal plane alignment in the treatment of spinal deformity.

There are some limitations to the present study, which might affect the conclusions drawn from its findings. Because validated patient-oriented instruments were not available 20 years ago, long-term assessment of this type of surgery must be retrospective. The response rate was low, as expected in a study with very-long-term follow-up evaluation. Unfortunately, since no control group of untreated patients with scoliosis was available, the final effect of operative procedure on the natural course of deformity could not be clearly determined, and the interpretation of the results of this study may be limited because of the multiple etiologies of scoliosis. However, no selection bias was found among the patients available for follow-up assessment in terms of either demographic or preoperative characteristics.

We evaluated outcome following scoliosis surgery for longer than 16 years. The results obtained in this study should be regarded as intermediate and further investi-

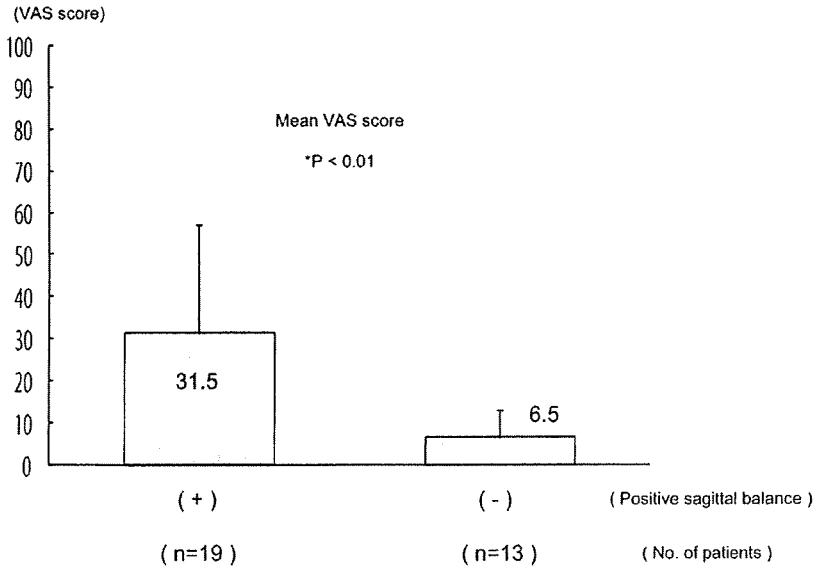

Figure 6. Correlation between positive sagittal balance and VAS score. Nineteen patients (59.4%) had positive sagittal balance, and their mean VAS score was significantly higher than that of the other patients (*$P < 0.01$).

gations with longer follow-up are needed to confirm the findings of this study, which are, however, important for both surgeons and patients.

■ Key Points

- We evaluated long-term outcomes regarding low back pain following scoliosis surgery.
- Regardless of residual back deformity, low back pain was no more frequent than in the normal population in this 21-year follow-up.
- Positive sagittal balance at the latest follow-up was a factor significantly contributing to low back pain following scoliosis surgery.

References

1. Danielsson AJ. What impact does spinal deformity correction for adolescent idiopathic scoliosis make on quality of life? *Spine* 2007;32:S101–8.
2. Moskowitz A, Moe JH, Winter RB, et al. Long-term follow-up of scoliosis fusion. *J Bone Joint Surg Am* 1980;62:364–76.
3. Strayer L, Risser J, Waugh T. Results of spinal fusion for scoliosis rwenty-five years or more after surgery. Paper presented at: Annual Meeting of the Scoliosis Research Society; September 1968; Houston, TX.
4. Van Grouw A Jr, Nadel CI, Weierman RJ, et al. Long term follow-up of patients with idiopathic scoliosis treated surgically: a preliminary subjective study. *Clin Orthop* 1976;117:197–201.
5. Lovallo JL, Banta JV, Renshaw TS. Adolescent idiopathic scoliosis treated by Harrigton rod distractione and fusion. *J Bone Joint Surg Am* 1986;68:1326–30.
6. Remes V, Helenius I, Schlenzka D, et al. Cotrel-Dubousset (CD) or Universal Spine System (USS) instrumentation in adolescent idiopathic scoliosis (AIS): comparison of mid-term clinical, functional, and radiologic outcomes. *Spine* 2004;29:2024–30.
7. Helenius I, Remes V, Yrjonen T, et al. Harrington and Cotrel-Dubousset instrumentation in adolescent idiopathic scoliosis: long-term functional and radiographic outcomes. *J Bone Joint Surg Am* 2003;85:2303–9.
8. Mariconda M, Galasso O, Barca P, et al. Minimum 20-year follow-up results of Harrington rod fusion for idiopathic scoliosis. *Eur Spine J* 2005;14:854–61.
9. Connolly PJ, Von Schroeder HP, Johnson GE, et al. Adolescent idiopathic scoliosis. Long-term effect of instrumentation extending to the lumbar spine. *J Bone Joint Surg Am* 1995;77:1210–16.
10. Dickson JH, Erwin WD, Rossi D. Harrington instrumentation and arthrodesis for idiopathic scoliosis. A twenty-one-year follow-up. *J Bone Joint Surg Am* 1990;72:678–83.
11. Cochran T, Irstam L, Nachemson A. Long-term anatomic and functional changes in patients with adolescent idiopathic scoliosis treated by Harrington rod fusion. *Spine* 1983;8:576–84.
12. Hayes MA, Tompkins SF, Herndon WA, et al. Clinical and radiological evaluation of lumbosacral motion below fusion level in idiopathic scoliosis. *Spine* 1988;10:1161–7.
13. Fabry G, Van Melkebeek J, Bockx E. Back pain after Harrington rod instrumentation for idiopathic scoliosis. *Spine* 1989;14:620–4.
14. Gotze C, Liljenqvist UR, Slomka A, et al. Quality of life and back pain: outcome 16.7 years after Harrington instrumentation. *Spine* 2002;27:1456–63; discussion 1463–4.
15. Padua R, Padua S, Aulisa L, et al. Patient outcomes after Harrington instrumentation for idiopathic scoliosis: a 15 to 28 year evaluation. *Spine* 2001; 26:1268–73.
16. Helenius I, Remes V, Yrjonen T, et al. Comparison of long-term functional and radiologic outcomes after Harrington instrumentation and spondylodesis in adolescent idiopathic scoliosis: a review of 78 patients. *Spine* 2002;27: 176–80.
17. Niemeyer T, Bovingloh AS, Grieb S, et al. Low back pain after spinal fusion and Harringron instrumentation for idiopathic scoliosis. *Int Orthop* 2005; 29:47–50.
18. Benli IT, Ates B, Akalin S, et al. Minimum 10 years follow-up surgical results of adolescent idiopathic scoliosis patients treated with TSRH instrumentation. *Eur Spine J* 2007;16:381–91.
19. Danielsson AJ, Nachemson AL. Back pain and function 23 years after fusion for adolescent idiopathic scoliosis: a case–control study-part II. *Spine* 2003; 28:E373–83.
20. Glassman SD, Bridwell K, Dimar JR, et al. The impact of positive sagittal balance in adult spinal deformity. *Spine* 2005;30:2024–9.
21. Weiner DK, Distell B, Studenski S, et al. Does radiographic osteoarthritis correlate with flexibility of the lumbar spine? *J Am Geriatr Soc* 1994;42: 257–63.
22. Bjerkreim I, Steen H, Brox JI. Idiopathic scoliosis treated with Cotrel-Dubousset instrumentation evaluation 10 years after surgery. *Spine* 2007; 32:2103–10.
23. Boos N, Dolan LA, Stuart L, et al. Long-term clinical and radiographic results of Cotrel-Dubousset instrumentation of right thoracic adolescent idiopathic scoliosis. *Iowa Orthop J* 2007;27:40–6.
24. Weinstein SL, Dolan LA, Spratt KF, et al. Health and function of patients with untreated idiopathic scoliosis: a 50-year natural history study. *JAMA* 2003;289:559–67.
25. Schwab FJ, Smith VA, Biserni M, et al. Adult scoliosis. A quantitative radiographic and clinical analysis. *Spine* 2002;27:387–92.
26. Buttermann GR, Mullin WJ. Pain and disability correlated with disc degeneration via magnetic resonance imaging in scoliosis patients. *Eur Spine J* 2008;17:240–9.
27. Gremeaux V, Casillas JM, Peray PF. Analysis of low back pain in adults with scoliosis. *Spine* 2008;33:402–5.
28. Tones M, Moss N, Polly DW. A review of quality of life and psychosocial issues in scoliosis. *Spine* 2006;26:3027–38.
29. Asher MA, Lai SM, Burton D, et al. The reliability and concurrent validity of the Scoliosis Research Society-22 patient questionnaire for idiopathic scoliosis. *Spine* 2003;28:63–9.

SPINE Volume 34, Number 24, pp E882–E885

Primary NK/T-Cell Lymphoma of the *Cauda Equina*

A Case Report and Literature Review

Masahiro Morita, MD,* Masahiko Osawa, MD, PhD,† Hirotsune Naruse, MD, PhD,‡ and Hiroaki Nakamura, MD, PhD§

Study Design. A case report with a review of the literature.

Objective. To describe an unusual case of primary lymphoma of the *cauda equina* and provide a review of the literature of this condition.

Summary of Background Data. Primary lymphoma of the cauda equina is extremely rare, and has been reported in 8 cases previously. This report is the first to describe a case of primary nasal type NK/T-cell lymphoma of the *cauda equina*.

Methods. We report the case of a 67-year-old man presenting the symptoms of cauda equina syndrome caused by primary lymphoma of the *cauda equina*.

Results. After laminectomy and removal of the tumor, the patient recovered from the symptoms of cauda equina syndrome except for bladder and bowel dysfunction. Further investigations including immunohistochemical stains made a diagnosis of primary nasal type NK/T-cell lymphoma of the *cauda equina*, and the patient received radiotherapy to the lumbosacral area. Brain metastasis was detected 8 months after surgery, and the patient died 14 months after his initial clinical presentation despite additional treatments including whole-brain radiotherapy and oral chemotherapy.

Conclusion. Although primary lymphoma of the cauda equina is extremely rare, the prognosis of this condition is thought to be poor. Early definitive diagnosis with examination of the cerebrospinal fluid followed by combined treatment with radiotherapy and high-dose methotrexate should be considered.

Key words: primary lymphoma, nasal type NK/T-cell lymphoma, *cauda equina*. **Spine 2009;34:E882–E885**

Spinal involvement is not uncommon in the advanced stage of malignant lymphoma. However, primary lymphoma of the spine has been reported to account for about one-third of all primary bone lymphomas which accounts for <5% of extranodal lymphomas and <2% of all lymphomas in adults.[1] Clinical manifestations of the disease may vary, and they may include back pain due to pathologic fractures, as well as leg symptoms, such as leg pain or motor weakness due to spinal cord compression. Spinal epidural involvement has been reported in 0.8% to 2.8% of all malignant lymphoma cases.[2]

On the other hand, primary central nervous system lymphoma is also an extranodal non-Hodgkin lymphoma that arises from the brain parenchyma, eyes, meninges, or spinal cord in the absence of systemic disease; the spinal cord is the rarest site of involvement in patients with this condition.[3] In addition, primary lymphoma of the *cauda equina* is extremely rare. The purpose of this article is to describe the detailed clinical and pathologic findings of an extremely rare case of nasal type NK/T-cell lymphoma that had a primary origin from the *cauda equina* with a review of the literature.

■ Case Report

A 67-year-old man was referred to our hospital with a 2-month history of severe leg pain as well as bladder and bowel dysfunction. The symptoms had progressed within a few weeks after onset, and he could not walk because of severe leg pain. Before the onset of symptoms, he had been in good general health. Physical examination revealed mild motor weakness in both lower extremities, predominantly affecting the distal muscles, bilateral absence of lower limb reflexes, and severe diminished pinprick and light touch sensation in his perineal region despite almost normal neurologic findings in his upper extremities and normal cranial nerve function. Routine hematological and biochemical tests, as well as Human Immunodeficiency virus serology, were normal. Magnetic resonance imaging of his lumbar spine revealed spinal canal stenosis at L4/5 and a mass lesion with an apparent intensity change occupying nearly the entire thecal sac from L3–L5, with nonmarked demarcation to the normal *cauda equina*. The mass had marked and homogeneous enhancement after intravenous injection of gadolinium-DTPA. A lumbar myelogram demonstrated complete block of the contrast medium at L3/4 (Figure 1). Magnetic resonance imaging of his brain and total spine revealed no evidence of other involvement. After bilateral laminectomy at L3–L5 and incision of the dural sac, the *cauda equina* was noted to be swollen and reddish-gray tumors were present. The tumors infiltrated extensively between the *cauda equina* and adhered strongly to the nerve root. The tumors were removed as far as possible with special attention not to damage the nerve root. After surgery, the patient's severe leg pain improved considerably, and he could walk without a cane or a walker, but bladder and bowel dysfunction still

From the *Department of Orthopaedic Surgery, Izumi Municipal Hospital, Izumi City, Osaka, Japan; †Department of Diagnostic Pathology, Osaka City University Graduate School of Medicine, Abeno, Osaka, Japan; ‡Department of Neurosurgery, Izumi Municipal Hospital, Izumi City, Osaka, Japan; and §Department of Orthopaedic Surgery, Osaka City University Graduate School of Medicine, Abeno, Osaka, Japan.

Acknowledgment date: November 23, 2008. First revision date: March 12, 2009. Acceptance date: April 6, 2009.

The manuscript submitted does not contain information about medical device(s)/drug(s).

No funds were received in support of this work. No benefits in any form have been or will be received from a commercial party related directly or indirectly to the subject of this manuscript.

Address correspondence and reprint requests to Masahiro Morita, MD, Department of Orthopaedic Surgery, Izumi Municipal Hospital, 4–10–10 Fuchu Izumi City Osaka, 594–0071, Japan; E-mail: m1908130@msic.med.osaka-cu.ac.jp

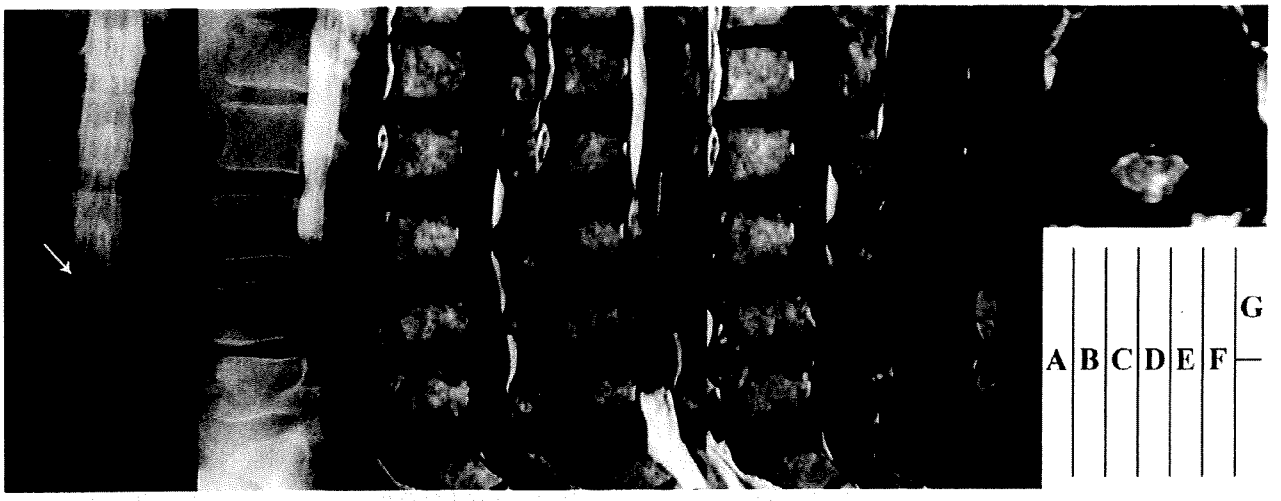

Figure 1. Myelography—(**A**) posteroanterior, (**B**) lateral—showing a complete block at L3/4, and nodular thickening of the lumbar nerve roots (arrow). Magnetic resonance imaging—(**C**) T1-weighted sagittal image, (**D**) T2-weighted sagittal image, (**E**) T1-weighted sagittal image with gadolinium enhancement, (**F**) T1-weighted and fat suppression sagittal image with gadolinium enhancement, (**G**) T1-weighted and fat suppression axial image with gadolinium enhancement at L4—showing an intrathecal mass at the lesion and marked enhancement with gadolinium.

remained. A diagnosis of nasal type NK/T-cell lymphoma of the *cauda equina* was made based on immunohistochemical stains. Further investigations, including gallium and technetium scintigraphy, thoracic, abdominal, and pelvic computed tomography, and bone marrow biopsy of the iliac bone, did not reveal any other site of lymphoma. The patient received radiotherapy to the lumbosacral area with a dose of 50 Gy after surgery but refused chemotherapy. A routine metastatic workup demonstrated unremarkable findings until he complained of clouding of consciousness, which was caused by brain metastasis 8 months after surgery. Despite whole-brain radiotherapy (30 Gy) and oral chemotherapy (etoposide), the patient died 14 months after his initial clinical presentation.

■ Pathologic Findings

The medium-sized and large-sized lymphoid cells with irregular nuclei showed diffuse proliferation among the necrotic nerve fibers in the *cauda equina* (Figure 2). Coagulative necrosis and angiocentric infiltration of lymphoma cells were also found in the tumor. The inflammatory cells, including neutrophils, macrophages, plasma cells, and eosinophils, were also intermingled. On immunohistochemistry, the lymphoma cells were positive for CD3 and CD56, detected by immunohistochemical method using monoclonal antibodies, anti-CD3 (PS1, Immunotech, Marseilla, France) and anti-CD56 (1B6, Nichirei Bioscience, Tokyo, Japan). Epstein Barr viral early RNA-1 was detected in the nucleus of the lymphoma cells by *in situ* hybridization, using the Epstein Barr viral early RNA-1 probe.

■ Discussion

Primary central nervous system lymphoma is an extranodal non-Hodgkin lymphoma that accounts for 5% to 7% of primary brain tumors and 1% to 2% of all cases of non-Hodgkin lymphoma.[4] The spinal cord is the rarest site of involvement in patients with primary central nervous system lymphoma, although meningeal dissem-

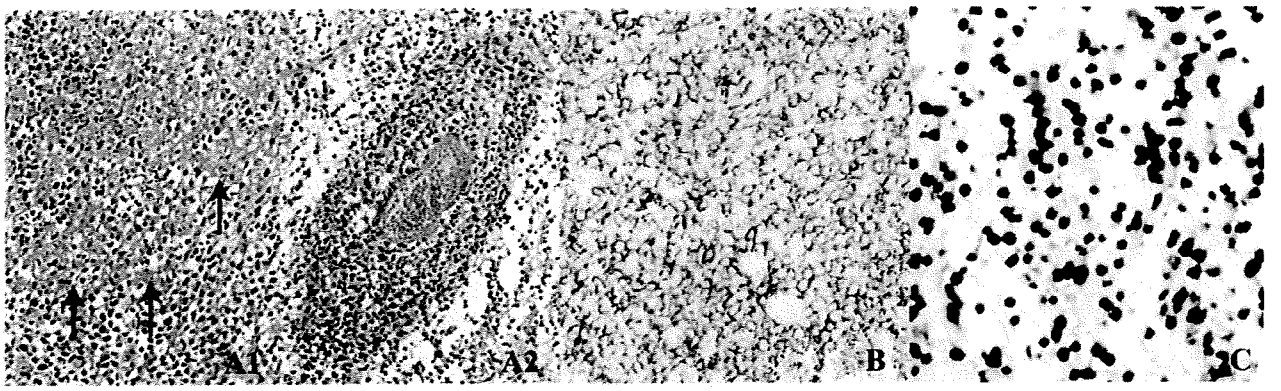

Figure 2. Diffuse proliferation of lymphoma cells with the coagulative necrosis of lymphoma cells (arrow) (**A-1**) and angiocentric pattern of lymphoid (**A-2**) infiltrate in the fascia of the cauda equina (hematoxylin-eosin stain). **B**, Lymphoma cells are positive for CD56. **C**, Epstein Barr virus was detected in the nucleus of lymphoma cells by Epstein Barr viral early RNA *in situ* hybridization. Magnification, ×350.

Table 1. Literature Review of Patients With Primary Lymphoma of the *Cauda Equina*

Reference	Age/Sex	Interval (Onset-Diagnosis)	Pathology	Treatment	Outcome	F/U
Mauney and Sciotto[6]	68/F	1 wk	B cell lymphoma	RT	Alive	3 mo
Toner *et al*[7]	59/M	3 mo	B cell lymphoma	RT, CT (Intrathecal and intravenous)	Alive	2 yr
Klein *et al*[8]	29/F	2 wk	B cell lymphoma	N.A.	Died	5 wk
Knopp *et al*[9]	69/F	3 wk	N.A.	N.A.	N.A.	N.A.
Ooi *et al*[10]	16/M	3 wk	T-lymphoblastic lymphoma	RT, CT (Intrathecal and intravenous)	Died	8 mo
Giobbia *et al*[11]	30/F	2 mo	B cell lymphoma	RT, CT (Intrathecal)	Alive	1 yr
Zagami and Granot[12]	71/F	3 wk	B cell lymphoma	CT (Intrathecal)	Died	16 mo
Tajima *et al*[13]	67/F	3 yr	B cell lymphoma	RT, CT (Intrathecal)	Alive	3 yr

N.A. indicates not available; RT, radiation therapy; CT, chemotherapy; F/U, duration of follow-up after onset.

ination to the spinal cord from an intracranial focus may sometimes occur at an advanced stage of systemic lymphoma. Although previous studies report that less than 1% of primary central nervous system lymphoma occur in the spinal cord,[5] the rate of primary lymphoma in the *cauda equina* has not been reported.

Based on our review of the English literature[6–13] (Table 1), only 8 cases of primary lymphoma of the *cauda equina* have been reported. A summary of the clinical course, imaging findings, and histologic findings of these reports is presented.

First, the symptoms of *cauda equina* syndrome, such as lower extremity paresthesia, muscular weakness, and bladder dysfunction, progress rapidly within a short period of time. Most cases, including the present case, presented with a few weeks history of progressive symptoms. Second, the *cauda equina* lesions show isointense or increased signals on T1-weighted magnetic resonance images and increased signals on T2-weighted images, along with no abnormal signal changes in the vertebrae. However, marked enhancement of the *cauda equina* lesions on gadolinium-DTPA-enhanced T1-weighted images is observed, which can be useful for identifying the lesions. A thickened *cauda equina* nerve root on magnetic resonance imaging after gadolinium-DTPA enhancement[8,12,13] or on myelography[7,8] is another imaging finding. Lastly, although Ooi *et al*[10] reported T-lymphoblastic primary lymphoma of the *cauda equina*, primary lymphoma of the *cauda equina* is predominantly non-Hodgkin lymphoma of the B-cell type.

The differential diagnosis of primary intradural tumors arising at the level of *cauda equina* (including conus region) consists mainly of neurofibromas, ependymomas, and schwannomas, and less commonly meningiomas, dermoids, epidermoids, paragangliomas, high grade gliomas, hemangioblastomas, and so on.[14]

Magnetic resonance imaging using gadolinium enhancement can usually suggest the nature of the tumor. Almost all tumors enhance, and gadolinium helps to separate the solid portion of tumors from adjacent edema and associated cysts.[15] Schwannomas demonstrate isointence on T1-weighted and hyperintence on T2-weighted magnetic resonance images, and usually have more irregular enhancement in comparison to meningiomas because of internal necrosis and/or cystic degeneration. Meningiomas demonstrate isointence on both T1- and T2- weighted magnetic resonance images and hyperintence on contrast enhanced, and ependymomas, which almost exclusively have a myxopathic histology at this level, demonstrate isointence on T1- weighted and hyperintence on T2-weighted magnetic resonance images and contrast enhanced.[14]

Other than open biopsy, definitive diagnosis using a cytocentrifuge preparation of the cerebrospinal fluid has been suggested; some authors have recommended routine cerebrospinal fluid evaluation.[6,16]

Optimal treatment for primary central nervous system lymphoma, which was previously treated with radiotherapy alone,[17] has not yet been established.[18] On the other hand, there are convincing data that high-dose methotrexate-based chemotherapy regimens provide better survival rates than radiotherapy alone.[19] However, the rates of permanent neurologic side effects following combined treatment with radiotherapy and high-dose methotrexate are unacceptably high in the elderly population.[17] As described in the present case report, primary lymphoma of the *cauda equina* should be differentiated even if there is no spinal involvement. As the prognosis with this lesion is not good, early definitive diagnosis with examination of the cerebrospinal fluid followed by combined treatment with radiotherapy and high-dose methotrexate should be considered.

■ Key Points

- The first case of primary nasal type NK/T-cell lymphoma of the *cauda equina* is reported.
- Optimal treatment for primary lymphoma of the *cauda equina* has not yet been established, and the prognosis of this condition is thought to be poor.
- Early definitive diagnosis with examination of the cerebrospinal fluid followed by combined treatment with radiotherapy and high-dose methotrexate should be considered.

References

1. Ramadan KM, Shenkier T, Sehn LH, et al. A clinicopathological retrospective study of 131 patients with primary bone lymphoma: a population-based

study of successively treated cohorts from the British Columbia Cancer Agency. *Ann Oncol* 2007;18:129–35.
2. Székely G, Miltényi Z, Mezey G, et al. Epidural malignant lymphomas of the spine: collected experiences with epidural malignant lymphomas of the spinal canal and their treatment. *Spinal Cord* 2008;46:278–81.
3. Eichler AF, Batchelor TT. Primary central nervous system lymphoma: presentation, diagnosis and staging. *Neurosurg Focus* 2006;21:1–9.
4. Iwamoto FM, DeAngelis LM. An update on primary central nervous system lymphoma. *Hematol Oncol Clin North Am* 2006;20:1267–85.
5. Hochberg FH, Miller DC. Primary central nervous system lymphoma. *J Neurosurg* 1988;68:835–53.
6. Mauney M, Sciotto CG. Primary malignant lymphoma of the cauda equina. *Am J Surg Pathol* 1983;7:185–190.
7. Toner GC, Holmes R, Sinclair RA, et al. Central nervous system lymphoma: primary lumber nerve root infiltration. *Acta Haematol* 1989;81:44–7.
8. Klein P, Zientek G, Vandenberg SR, et al. Primary CNS lymphoma: lymphomatous meningitis presenting as a cauda equina lesion in an AIDS patient. *Can J Neurol Sci* 1990;17:329–31.
9. Knopp EA, Chynn KY, Hughes J. Primary lymphoma of the cauda equina: myelographic, CT myelographic, and MR appearance. *AJNR Am J Neuroradiol* 1994;15:1187–9.
10. Ooi GC, Peh WC, Fung CF. Case report: magnetic resonance imaging of primary lymphoma of the cauda equina. *Br J Radiol* 1996;69:1057–60.
11. Giobbia M, Carmato A, Scotton PG, et al. Primary EBV-associated cauda equina lymphoma. *J Neurol* 1999;246:739–40.
12. Zagami AS, Granot R. Non-Hodgkin's lymphoma involving the cauda equina and ocular cranial nerves: case reports and literature review. *J Clin Neurosci* 2003;10:696–9.
13. Tajima Y, Sudo K, Matumoto A. Malignant lymphoma originating in the cauda equina mimicking the inflammatory polyradiculoneuropathy. *Intern Med* 2007;46:1029–32.
14. Kotil T, Bilge T. Primary intradural conus and cauda equina tumors: long-time outcome with 14 years follow-up. *Turkish Neurosurgery* 2006;16:130–8.
15. Mathew P, Todd NV. Intradural conus and cauda equina tumours: a retrospective review of presentation, diagnosis and early outcome. *J Neurol Neurosurg Psychiatry* 1993;56:69–74.
16. MacKintosh FR, Colby TV, Podolsky WJ, et al. Central nervous system involvement in non-Hodgkin's lymphoma: an analysis of 105 cases. *Cancer* 1982;49:586–95.
17. DeAngelis LM, Iwamoto FM. An update on therapy of primary central nervous system lymphoma. *Hematology Am Soc Hematol Educ Program* 2006;311–6.
18. Yamanaka R, Morii K, Shinbo Y, et al. Results of treatment of 112 cases of primary CNS lymphoma. *Jpn J Clin Oncol* 2008;38:373–80.
19. Ferreri AJ, Abrey LE, Blay JY, et al. Summary statement on primary central nervous system lymphoma from the Eighth International Conference on malignant lymphoma, Lugano, Switzerland, June 12 to 15, 2002. *J Clin Oncol* 2003;21:2407–14.

Knee Surg Sports Traumatol Arthrosc
DOI 10.1007/s00167-009-0927-5

KNEE

The risk of notching the anterior femoral cortex with the use of navigation systems in total knee arthroplasty

Yukihide Minoda · Akio Kobayashi · Hiroyoshi Iwaki · Ikebuchi Mitsuhiko · Yoshinori Kadoya · Hirotsugu Ohashi · Kunio Takaoka · Hiroaki Nakamura

Received: 8 June 2009 / Accepted: 8 September 2009

Abstract Use of navigation systems has recently been introduced in total knee arthroplasty (TKA) to achieve more reliable prosthetic alignment. In the sagittal plane, there are two important requirements for navigation systems: (1) perpendicular cut to the femoral mechanical axis and (2) prevention of notching of anterior femoral cortex. These two requirements, however, may conflict. The angles between the line of the anterior femoral cortex and four sagittal femoral mechanical axes for navigation systems using radiographs of the entire lower extremity, while standing were measured and compared. These four sagittal axes simulated on the radiographs in navigation systems were in extension relative to the line of the anterior femoral cortex in 40–85% of cases in male and 65–100% in elderly female. The present study showed that navigation systems have the potential risk for notching of anterior femoral cortex.

Y. Minoda (✉) · A. Kobayashi · H. Iwaki · I. Mitsuhiko · K. Takaoka · H. Nakamura
Department of Orthopaedic Surgery, Osaka City University Graduate School of Medicine, 1-4-3 Asahi-machi, Abeno-ku, Osaka 545-8585, Japan
e-mail: yminoda@msic.med.osaka-cu.ac.jp

A. Kobayashi
Department of Orthopaedic Surgery, Osaka General Medical Center, 3-1-56 Mandai-higashi, Sumiyoshi-ku, Osaka 558-8558, Japan

Y. Kadoya
Department of Orthopaedic Surgery, Osaka Rosai Hospital, 1179-3 Nagasone-cho, Sakai City, Osaka 591-8025, Japan

H. Ohashi
Department of Orthopaedic Surgery, Saiseikai Nakatsu Hospital, 2-10-39 Shibata, Kitaku, Osaka 530-0012, Japan

Published online: 26 September 2009

Keywords Total knee arthroplasty · Navigation system · Notching of anterior femoral cortex

Introduction

Alignment of the prosthesis is one of the most important factors in the longevity of total knee arthroplasty (TKA). It has been reported that passage of the mechanical axis through the center of the prosthesis is preferable for long-term clinical success of TKA [2, 10, 18, 21, 23]. To provide more reliable alignment and to reduce the number of outliers of the femoral and tibial component alignment relative to the mechanical axis, navigation systems have recently been introduced in TKA [1, 4, 6, 8, 11, 13, 17, 19, 20]. Using navigation systems, alignment of the femoral component, i.e., the distal femoral bone cut surface, is planned to be perpendicular to the femoral mechanical axis, which passes through the center of the femoral head and the reference point on the distal femoral condyle. Although the center of the distal femoral condyle is considered to be the reliable reference point in the coronal plane, the reliable reference point on the distal femoral condyle in the sagittal plane is still controversial [16]. A previous report showed that sagittal femoral mechanical axis for navigation systems varies significantly according to the reference point on the distal femoral condyle [16]. Apart from the sagittal mechanical axis, notching of anterior femoral cortex should be avoided because notching of anterior femoral cortex contributes to complication such as postoperative femoral fracture [12, 24]. Therefore, when navigation systems are used, there are two important requirements in the sagittal plane: (1) perpendicular cut of distal femoral condyle to the femoral mechanical axis, and (2) prevention of notching of anterior femoral cortex. These two requirements, however,

may conflict. The purpose of this study was to simulate the sagittal alignment targeted by navigation systems using lateral radiographs of the whole lower extremity and to determine if navigation systems resulted in notching of anterior femoral cortex.

Materials and methods

Lateral radiographs of all 40 lower limbs were obtained from 10 male Japanese volunteers (mean age, 27 years [range, 24–31 years]) who had no pain, history of trauma, or radiographic abnormalities in lower extremities and from 10 Japanese (mean age, 75 years [range, 62–85 years]) who had no history of operation in lower extremities and planned to have TKA due to osteoarthritis of the knee joint. The mean height and body weight of male volunteers were 172 cm (range, 160–178 cm) and 68 kg (range, 52–90 kg), respectively. The mean height and body weight of female TKA candidates were 148 cm (range, 138–154 cm) and 55 kg (range, 45–66 kg), respectively. Using lateral radiographs of the whole lower extremity in one-legged stance, the sagittal femoral axes for TKA with the navigation systems and the tangent line to anterior cortex of the distal femur were simulated. If mechanical axis for navigation systems is in extension relative to the line tangent to anterior femoral cortex, navigation systems have the risk of notching of anterior femoral cortex. Therefore, the relationship between these lines was evaluated. Each gave informed consent to participate in this study, which was approved by our Institutional Review Board.

Lateral radiographs of the lower extremity in the one-legged stance were obtained using the previously validated technique [15, 16]. Film size 252 × 905-mm (SR-G; Konica, Tokyo, Japan) and a screen (LC-S3; Toshiba, Tokyo, Japan) were used. The X-ray beam was centered at the knee joint level at a distance of 200 cm. A grid (film-focus distance: 130 cm-∞, grid ratio: 6:1, grid line: 34/cm) (Mitaya Co., Tokyo, Japan) was used. The settings of the X-ray beam were 90 kV and 20–40 mA s for lateral radiographs, depending upon limb size. The subject was positioned in the following manner [15, 16]: (1) the knee was fully extended in weight bearing; (2) subjects were instructed to face laterally so the posterior edges of the medial and lateral femoral condyles were aligned; and (3) a graduated, lead-loaded acrylic filter (0.2 mpb) was placed in front of the collimated X-ray beam for lateral radiographs so the femoral head received highenergy exposure with the knee and ankle receiving relatively low-energy exposure. If both posterior condyles were not aligned, another radiograph was taken.

The following lines on the lateral radiographs were defined to evaluate the relationship between various sagittal femoral mechanical axes for navigation systems and anterior femoral notching.

Anterior cortex line of the femur (AC line) (Fig. 1)

The line tangent to anterior cortex of the distal femur at 7 cm proximal to the joint line was defined as the AC line (Fig. 1), since the distance from the top of the anterior flange to the bottom of the femoral condyle with the usual size of femoral component for Japanese individuals is 7 cm.

Sagittal femoral axes with navigation systems (Fig. 2) [16]

For navigation systems, the sagittal femoral axes were defined as the lines from the center of the femoral head to the following four points:

1. The point of insertion of the intra-medullary guide rod. The direction of the intra-medullary guide rod was defined as the line through the center of the femoral

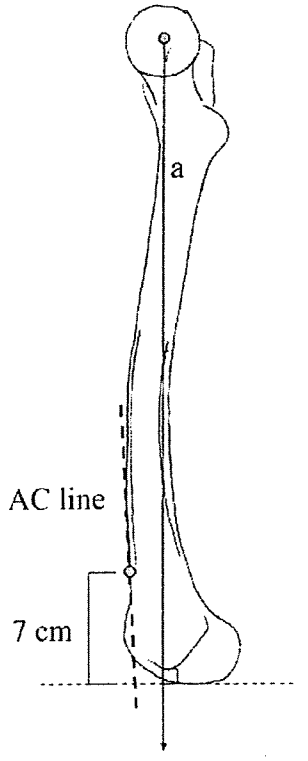

Fig. 1 The diagram shows AC line of the femur in the sagittal plane. The tangent to anterior cortex of distal femur at 7 cm proximal from the *joint line* is defined as the AC line. (*a*) Sagittal mechanical axis of the entire lower extremity, which is the *line* drawn from the center of the femoral head to the center of the talocrural joint

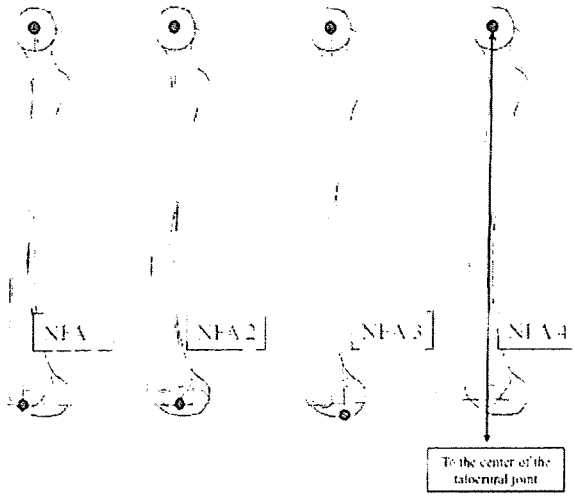

Fig. 2 The diagrams show four sagittal femoral mechanical axes for navigation systems. *NFA* navigation femoral axis

canal at 10 and 20 cm proximal to the distal femoral condyle (Navigation femoral axis 1 [NFA 1]).
2. The center of the femoral condyle (NFA 2).
3. The most distal point of the femoral condyle (NFA 3). If the most distal points of the medial and lateral femoral condyles were not same, the midpoint between the most distal points of the medial and the lateral femoral condyles was used.
4. The center of the talocrural joint (NFA 4).

The angle between the AC line and four sagittal femoral mechanical axes for navigation systems (NFA 1–4) was measured using computer software (Quick Grain Standard; Inotech, Hiroshima, Japan) and calculated to two decimal places. Female TKA candidates could not fully extent their knees due to flexion contracture. Therefore, NFA 4 was not measured in the female group. If the NFA was in extension relative to the AC line, it was defined as "notching positive," and the angle was assigned positive values, whereas if it was in flexion, it was defined as "notching negative," and the angle was assigned negative values (Fig. 3A, B).

Statistical analysis

The angles between AC line and reference lines (NFA 1–3) were compared between groups using student *t* test. The Fisher's exact test was performed to compare the rate of notching positive between the two groups.

Intraobserver and interobserver analysis

Previous report assessed interobserver and intraobserver variability for each measurement using 10 cases [16]. Intraobserver analysis indicated mean differences of 0.11°–0.42° in each parameter. Interobserver analysis indicated mean differences of 0.16°–0.44° in each parameter. Bland–Altman method [3] showed that intarobserver and interobserver reliabilities of each parameter were high.

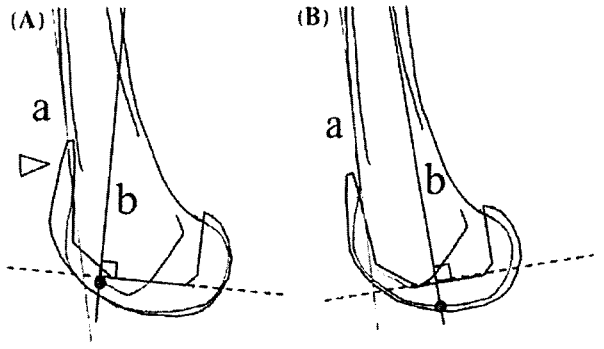

Fig. 3 The diagrams show the relationship between the AC line and NFA. **A** If the NFA was in extension relative to the AC line, we defined it as "notching positive" (*arrow*) and the angle between the AC line and the NFA was assigned positive value. **B** If the NFA was in flexion, we defined it as "notching negative," and the angle was assigned negative value. (*a*) AC line. (*b*) NFA

Results

The relationships between the AC line and the four sagittal femoral mechanical axes for navigation systems are shown in Table 1. The angle between the AC line and the two reference lines (NFA 1 and NFA 2) was statistically larger in female group than in male volunteer group ($P < 0.05$). The number of cases that was "notching positive" (positive values) in male volunteer group was 17 of 20 for NFA 1, 8 of 20 for NFA 2 and NFA 3, and 14 of 20 for NFA 4. The number of cases that was "notching positive" in female group was 20 of 20 for NFA 1, 14 of 20 for NFA 2, and 13 of 20 for NFA 3. However, the difference of notching cases was not statistically significant in NFA 1, NFA 2, or NFA 3 between two groups. If the 3° tilt of anterior flange of the femoral component is considered, the number of "notching positive" cases, in which the angle between NFA and AC line was greater than 3°, decreased. However, there were still several cases of notching using navigation systems for TKA in both groups (Table 1). The number of notching cases in NFA 1 and NFA 2 was larger in female group than in male volunteer group ($P < 0.05$).

Discussion

The most important finding of the present study is that there is the potential risk of notching of anterior femoral cortex using navigation systems for TKA in both male and female

Table 1 The relationship between AC line and four sagittal femoral mechanical axes for navigation systems

Parameter	Reference lines	Male volunteer group ($n = 20$)	Female group ($n = 20$)	P value
Angle between AC line and reference lines (°)[a]	NFA 1	1.7 ± 0.4 (−2.6 to 4.8)	3.9 ± 0.6 (−2.6 to 4.8)	0.003
	NFA 2	−0.1 ± 0.4 (−3.7 to 3.2)	2.6 ± 0.6 (−3.7 to 3.2)	0.001
	NFA 3	−0.7 ± 0.4 (−4.6 to 2.2)	0.7 ± 0.6 (−4.6 to 2.2)	NS
	NFA 4	1.0 ± 0.4 (−2.2 to 4.4)	-	
Number of "notching positive" cases	NFA 1	17/20	20/20	NS
	NFA 2	8/20	14/20	NS
	NFA 3	8/20	13/20	NS
	NFA 4	14/20	-	
Number of "notching positive" cases[b]	NFA 1	5/20	14/20	0.004
	NFA 2	1/20	9/20	0.008
	NFA 3	0/20	3/20	NS
	NFA 4	3/20	-	

NS not significant

[a] If the NFA was in extension relative to the AC line, degrees were assigned positive values, while if the NFA was in flexicon relative to the AC line, degrees were assigned negative values. Mean and standard error (range) were provided

[b] 3° tilt of anterior flange of femoral component was considered

groups. In some subjects, two of the requirements for navigation systems for TKA, perpendicular cut of the distal femoral condyle to the femoral mechanical axis and prevention of notching of the anterior femoral cortex, theoretically conflicted. The risk of notching was highest when the point of insertion of the intra-medullary guide rod (NFA 1) was chosen as the reference point on the distal femoral condyle. The present study also revealed that female group showed higher risk of notching than male volunteer group. It might be because that elderly females who planned to have TKA have shorter and more anteriorly bowed femurs [19]. Anterior bow of femur makes AC line in more extended position to sagittal mechanical axis of the femur.

At the moment, there are two major types of navigation systems for TKA, CT-based and CT-free systems. Reliable implant alignment can be obtained using each of these types of systems [1, 4, 6, 8, 11, 13, 17, 19, 20]. For CT-based navigation systems, preoperative CT of the entire lower extremity is required. Three-dimensional planning of implant alignment on CT data is performed before operation. In the operating room, the surgeon reproduces the plan of implant alignment using optical instruments. Because CT-based navigation systems have the step such as three-dimensional computerized planning, surgeon can check if navigation system leads anterior notching or not before operation and can re-adjust the mechanical axis not to make notching. On the other hand, CT-free navigation systems do not have such preoperative planning that warns of notching. Therefore, CT-free navigation system inherently has the risk of notching of the anterior femoral cortex. Recently, combined use of navigation systems and minimal incision surgery for TKA has been introduced [5, 22]. The disadvantage of restricted visualization in the minimal incision surgery was expected to be compensated by a navigation system [9]. However, the results of this study suggested that combined use of minimal incision surgery and navigation systems, especially for CT-free systems, should be used with great care to notching of anterior femoral cortex.

There were limitations in the current study. First, the evaluation performed in this study was 2D. Therefore, the rotation of femoral component could not be considered. The lateral radiographs were taken parallel to the posterior condylar line. Thus, this study simulated the risk of notching when femoral component was implanted parallel to posterior condylar line. However, femoral component is usually implanted in slightly externally rotated position relative to posterior condylar line [7]. It has been reported that more externally rotated implantation of femoral component has higher risk of notching of anterior femoral cortex [14]. Therefore, the risk of notching in clinical situation might be higher than that in the simulation of this study using two-dimensional evaluation. Second, the present study is not a clinical study, but an experimental study. Notching of anterior femoral cortex is considered to be one of the risk factors of postoperative femoral fracture [12, 24]. From the point of view of ethics, it is difficult to determine if navigation systems do result in notching of anterior femoral cortex during the operation.

Conclusion

The present study showed that navigation systems for TKA have the potential risk of notching of the anterior femoral

cortex. Surgeons and technicians using navigation systems for TKA should be aware of this risk.

References

1. Bathis H, Perlick L, Tingart M et al (2004) Alignment in total knee arthroplasty. A comparison of computer-assisted surgery with the conventional technique. J Bone Joint Surg Br 86:682–687
2. Berger RA, Rubash HE, Seel MJ et al (1993) Determining the rotational alignment of the femoral component in total knee arthroplasty using the epicondylar axis. Clin Orthop Relat Res 286:40–47
3. Bland JM, Altman DG (1986) Statistical methods for assessing agreement between two methods of clinical measurement. Lancet 1(8476):307–310
4. Bolognesi M, Hofmann A (2005) Computer navigation versus standard instrumentation for TKA: a single-surgeon experience. Clin Orthop Relat Res 440:162–169
5. Bonutti PM, Dethmers DA, McGrath MS et al (2008) Navigation did not improve the precision of minimally invasive knee arthroplasty. Clin Orthop Relat Res 466:2730–2735
6. Chauhan SK, Clark GW, Lloyd S et al (2004) Computer-assisted total knee replacement. A controlled cadaver study using a multi-parameter quantitative CT assessment of alignment (the Perth CT protocol). J Bone Joint Surg Br 86:818–823
7. Clarke HD, Hentz JG (2008) Restoration of femoral anatomy in TKA with unisex and gender-specific components. Clin Orthop Relat Res 466:2711–2716
8. Haaker RG, Stockheim M, Kamp M et al (2005) Computer-assisted navigation increases precision of component placement in total knee arthroplasty. Clin Orthop Relat Res 433:152–159
9. Hart R, Janecek M, Cizmár I et al (2006) Minimally invasive and navigated implantation for total knee arthroplasty: X-ray analysis and early clinical results. Orthopade 35:552–557
10. Jeffery RS, Morris RW, Denham RA (1991) Coronal alignment after total knee replacement. J Bone Joint Surg Br 73:709–714
11. Jenny JY, Clemens U, Kohler S et al (2005) Consistency of implantation of a total knee arthroplasty with a non-image-based navigation system: a case–control study of 235 cases compared with 235 conventionally implanted prostheses. J Arthroplasty 20:832–839
12. Lesh ML, Schneider DJ, Deol G et al (2000) The consequences of anterior femoral notching in total knee arthroplasty. A biomechanical study. J Bone Joint Surg Am 82:1096–1101
13. Lützner J, Krummenauer F, Wolf C et al (2008) Computer-assisted and conventional total knee replacement: a comparative, prospective, randomised study with radiological and CT evaluation. J Bone Joint Surg Br 90:1039–1044
14. Middleton FR, Palmer SH (2007) How accurate is Whiteside's line as a reference axis in total knee arthroplasty? Knee 14:204–207
15. Minoda Y, Kobayashi A, Iwaki H et al (2008) Sagittal alignment of the lower extremity while standing in Japanese male. Arch Orthop Trauma Surg 128:435–442
16. Minoda Y, Kobayashi A, Iwaki H et al (2009) TKA sagittal alignment with navigation systems and conventional techniques vary only a few degrees. Clin Orthop Relat Res 467:1000–1006
17. Mizu-uchi H, Matsuda S, Miura H et al (2008) The evaluation of post-operative alignment in total knee replacement using a CT-based navigation system. J Bone Joint Surg Br 90:1025–1031
18. Oswald MH, Jakob RP, Schneider E et al (1993) Radiological analysis of normal axial alignment of femur and tibia in view of total knee arthroplasty. J Arthroplasty 8:419–426
19. Sparmann M, Wolke B, Czupalla H et al (2003) Positioning of total knee arthroplasty with and without navigation support. A prospective, randomised study. J Bone Joint Surg Br 85:830–835
20. Stulberg SD (2003) How accurate is current TKR instrumentation? Clin Orthop Relat Res 416:177–184
21. Tew M, Waugh W (1985) Tibiofemoral alignment and the results of knee replacement. J Bone Joint Surg Br 67:551–556
22. Tria AJ Jr (2006) The evolving role of navigation in minimally invasive total knee arthroplasty. Am J Orthop 35(7 Suppl):18–22
23. Wasielewski RC, Galante JO, Leighty RM et al (1994) Wear patterns on retrieved polyethylene tibial inserts and their relationship to technical considerations during total knee arthroplasty. Clin Orthop Relat Res 299:31–43
24. Zalzal P, Backstein D, Gross AE et al (2006) Notching of the anterior femoral cortex during total knee arthroplasty characteristics that increase local stresses. J Arthroplasty 21:737–743

Clin Orthop Relat Res (2009) 467:3206–3212
DOI 10.1007/s11999-009-0960-1

SYMPOSIUM: TRIBUTE TO DR. MARSHALL URIST: MUSCULOSKELETAL GROWTH FACTORS

Successful Spinal Fusion by E. coli-derived BMP-2-adsorbed Porous β-TCP Granules

A Pilot Study

**Sho Dohzono MD, Yuuki Imai MD, PhD,
Hiroaki Nakamura MD, PhD, Shigeyuki Wakitani MD, PhD,
Kunio Takaoka MD, PhD**

Published online: 7 July 2009

Abstract Bone morphogenetic proteins (BMPs) were originally identified as osteoinductive proteins. With cloning of BMP genes, studies of BMPs and their clinical application have advanced. However, with increasing clinical applications, drug delivery systems and production costs have become more important issues. To address these issues, we asked whether E. coli-derived rhBMP-2 (E-BMP-2)-adsorbed porous β-TCP granules could achieve posterolateral lumbar fusion in a rabbit model similar to autogenous bone grafts. Lumbar spinal fusion masses were evaluated by 3-D computed tomography, mechanical testing, and histological analyses 8 weeks after surgery. By these measures E-BMP-2-adsorbed β-TCP granules achieved lumbar spinal fusion in dose-dependent fashion in a rabbit model as well as autogenous bone graft. Our preliminary findings suggest E-BMP-2-adsorbed porous β-TCP could be a novel, effective alternative to autogenous bone grafting for generating new bone and promoting regenerative repair of bone, and potentially utilizable in the clinical setting for treating spinal disorders.

Each author certifies that he or she has no commercial associations (eg, consultancies, stock ownership, equity interest, patent/licensing arrangements, etc) that might pose a conflict of interest in connection with the submitted article. This work was supported in part by Grants-in-Aid from the Ministry of Education, Culture, Sports, Science, and Technology of Japan (Project Grants 16109009 and 1679085 to KT, and 19791018 to YI).
Each author certifies that his or her institution has approved the animal protocol for this investigation and that all investigations were conducted in conformity with ethical principles of research.

S. Dohzono, Y. Imai (✉), H. Nakamura, S. Wakitani, K. Takaoka
Department of Orthopaedic Surgery, Osaka City University Graduate School of Medicine, 1-4-3 Asahimachi, Abeno-ku, Osaka, Osaka 545-8585, Japan
e-mail: imai@med.osaka-cu.ac.jp

Introduction

Autogenous bone grafting from the iliac bone has commonly been used clinically to promote bone formation, such as in fusion of the unstable spine, repair of large bone defects, and treatment of pseudarthrosis. However, autogenous bone grafting has several disadvantages, including acute and/or chronic pain or dysesthesia, potential risk of wound infection, unsightly scars, and deformity at the donor site [4, 19]. Limited available mass of graft bone is an additional disadvantage, especially in cases of large augmentation and long fusion after correction of scoliosis. To avoid these problems various authors have proposed new materials or agents that can substitute for autogenous bone grafts, such as bioabsorbable polymers, hyaluronic acid, and others [3, 30, 35].

The use of BMPs with their osteoinductive properties [39] has long been considered a promising means of producing such bone graft substitutes. This concept, however, was practically realized after successful cloning of cDNAs of BMPs [42]. Recombinant BMPs (BMP-2 and BMP-7) are currently utilized in combination with bovine collagen carrier in clinical practice to treat skeletal disorders such as open fracture, anterior interbody fusion, and posterolateral lumbar fusion [1, 2, 5–11, 13–17, 20, 22, 23, 25, 26, 31, 34, 41]. However, problems remain with the use of animal-derived collagen, including the risk of generation of antibody or disease transmission and lack of mechanical strength of the carrier collagen. Implants incorporating BMP are also expensive owing to the need for high doses of BMP-2 and would be a barrier to widespread use of such

implants. Safe and cost-effective local delivery systems for BMPs avoiding these problems would be important. Better delivery systems and/or ways to reduce the required BMP dose by enhancing BMP action [24, 27, 33, 38] are possible solutions. At the same time, it is important to reduce the cost of production of recombinant human BMP-2 for widespread clinical use of rhBMP-2. The efficiency of production of BMP-2 with E. coli [18, 29] appears superior to that with animal cells, and might provide less expensive BMP-2 for practice use.

We therefore asked whether E. coli-derived rhBMP-2 (E-BMP-2)-adsorbed porous β-TCP granules could achieve posterolateral lumbar fusion in a rabbit model similar to autogenous bone graft as judged by radiographic fusion, mechanical stiffness and histologically evident fusion mass.

Materials and Methods

We used 68 New Zealand white rabbits 18 weeks of age (weight, 2.8–3.2 kg) in this experimental study. Of these, 52 rabbits were equally divided into four groups (13 per group) by dose of E-BMP-2 adsorbed to β-TCP granules (Table 1). Eight rabbits were used as negative controls (implantation of β-TCP granules alone without E-BMP-2) and the remaining eight had only autogenous bone grafting. Posterolateral lumbar spinal fusion was performed with autogenous bone or β-TCP granules adsorbed with five different doses of E-BMP-2. Efficacy of E-BMP-2 for lumbar spinal fusion was evaluated with CT for new bone formation and with fusion scores, the bending load of the fusion required to create 1-mm middle-span deflection, and histological examination with von Kossa staining for mineralization, toluidine blue and TRAP staining for cartilage formation and β-TCP resorption. This protocol including animal care was approved by the Institutional Committee for Animal Care and Experiments of Osaka City University Medical School.

Table 1. Implant assignment

Group	Total number	Number harvested		E-BMP-2 (μg/side)	β-TCP (μg/side)
		At 4 weeks	At 8 weeks		
Autogenous bone graft	8	0	8	–	–
BMP0	8	0	8	0	500
BMP5	13	5	8	5	500
BMP15	13	5	8	15	500
BMP50	13	5	8	50	500
BMP150	13	5	8	150	500

E-BMP-2 with dimeric molecular structure was produced in human BMP-2 gene-transfected E. coli with monomeric structure and stored in inclusion bodies, which were collected. The molecular structure was unfolded in protein-denaturing agents, and then refolded to form dimeric E-BMP-2 by removal of denaturing agents. Dimeric E-BMP-2 was purified by several steps of chromatography. Details of the procedures for dimerization of cytokines have already been reported [29, 40].

We anesthetized the animals with an intramuscular injection of ketamine (30 mg/kg) and xylazine (10 mg/kg). Flomoxef sodium (60 mg) was administered intramuscularly as a prophylactic antibiotic. Each rabbit underwent a single-level posterolateral intertransverse process fusion at L5–L6. We made a dorsal midline skin incision followed by two paramedian fascial incisions on both sides. The intermuscular plane between the multifidus and longissimus muscles was retracted to expose both transverse processes of L5–L6 and the intertransverse membranes. We used an electric-driven burr (Stryker, Kalamazoo, MI) to decorticate the posterior cortex of the transverse processes, and one of the implant or transplant materials was implanted in both sides (one implant per side). The wounds were then closed with 3–0 nylon sutures and skin staples. After surgery, rabbits had free access to food and water the same as before surgery.

To create the implants, E-BMP-2 freeze-dried powder was dissolved in distilled water to reconstitute before use. We used interconnecting porous β-TCP granules 1 mm to 3 mm in diameter (pore size, 50–350 μm; porosity, 75%) (HOYA Corp, Tokyo, Japan). To prepare one implant to bridge the sides between transverse processes of L5 and L6, 500 mg of β-TCP granules were soaked in 500 μl of distilled water containing one of various dosages of E-BMP-2 (5, 15, 50, or 150 μg) for more than 15 minutes at room temperature. Implants with 500 mg of β-TCP granules soaked with 500 μl of distilled water without E-BMP-2 served for controls. Adsorbance of β-TCP was established by determining the concentration of protein in supernatant after centrifugal separation using Bio-Rad protein assay dye reagent concentrate (Bio-Rad Laboratories, Inc., Hercules, CA). Based on the results of preliminary experiments, it was estimated less than 10% of E-BMP-2 was collected from the supernatant. Autogenous bone chips harvested from the iliac crest (0.8–1 g/side) were also prepared as positive controls.

Four weeks after surgery, five animals from each group were sacrificed by overdose of pentobarbital sodium (50 mg/kg), and the L4–L7 lumbar spines were harvested and processed for further examination. At 8 weeks after surgery, the remaining animals from the experimental and control groups (eight animals per group) were sacrificed and processed in the same fashion.

The lumbar spines were examined for fusion mass condition by anteroposterior plain radiography and CT (GE Yokogawa Medical System, Tokyo, Japan) at 1-mm slice thickness to construct 3-D images every 2 weeks and harvested with dissection of soft tissue at each time point. Fusion was evaluated on sagittal CT view 10 mm lateral from the midline. Three independent observers (SD, TM and HY), who were all spine surgeons, judged the fusions using the following standardized scale: 0 = no bone formation and of β-TCP or transplanted bone absorption between transverse processes, 1 = some bone formation between transverse processes, but β-TCP or transplanted bone absorption was incomplete, 2 = continuous bone bridging between transverse processes and β-TCP or transplanted bone absorption was complete. All three observers agreed on all observations.

Mechanical testing to evaluate the solidity of the L5–L6 fusion site was performed by a three-point flexion-bending test using a materials testing machine (Instron 5882, Instron, Boston, MA). The superior and inferior ends of samples were flattened by trimming, and samples were horizontally held in the apparatus. Three-point bending tests were performed with a 30-mm intersupport distance and a 1 mm/minute head speed. The bending load at 1-mm middle-span deflection was determined from the load-deflection curves.

The specimens harvested at 8 weeks (n = 3 from each group) after surgery were fixed in 4% paraformaldehyde overnight at 4°C, dehydrated in a graded ethanol series, and embedded in plastic resin. Sections 7 μm in thickness in the region of the intertransverse process were cut in the sagittal plane with a tungsten blade using a rotary microtome (RM2255, Leica Microsystems, Wetzlar, Germany) and stained with hematoxylin and eosin (H-E) after decalcification with 0.5 M EDTA for 30 minutes at room temperature, and stained with toluidine blue and von Kossa and van Gieson staining without decalcification. We examined four sections from each sample taken 10 mm lateral from the midline. Amounts of β-TCP in new bone were observed microscopically; area of residual β-TCP were identified manually using software specialized for bone histomorphometry, OsteoMeasure (Osteometrics Inc, Decatur, GA), and expressed per square micron (μm^2). To identify osteoclasts that might have resorbed β-TCP within newly formed bone masses, tartrate-resistant acid phosphatase (TRAP) staining was performed on three sections from specimens taken from each of the five groups of animals sacrificed at 4 weeks after implantation.

We determined differences in the radiographic score, bending load, and histomorphometric measures between the autogenous bone graft group and each of the four E-BMP-2 treatment groups using the Kruskal-Wallis test and the post-hoc Scheffe test. We used StatView-J 5.0 (SAS Institute Inc, CA, USA) for all analyses.

Results

E-BMP-2-adsorbed porous β-TCP granules achieved posterolateral lumbar fusion same as autogenous bone graft evaluated by 3-D CT images (Fig. 1A) and plain radiographs (data not shown). The β-TCP granules appeared replaced by calcified mass with flat surface in E-BMP-2 dose- and time-dependent fashion, though β-TCP granules of the control group without E-BMP-2 continued to be observed throughout the observation period. Moreover, the radiographic scores showed treatment with 15 μg/side of E-BMP-2 achieved spinal fusion similar to autogenous bone graft, and that higher scores were obtained with 50 and 150 μg/side of E-BMP-2 than for the autogenous bone graft control (Fig. 1B).

The bending load required to produce 1-mm middle-span deflection of the fusion mass for the BMP15 group was similar to that of the autogenous bone graft control group (Fig. 2). The bending load of the specimens from the BMP50 and BMP150 groups were higher than those in the autogenous bone graft control group (Fig. 2). Specimens from animals with the β-TCP granules retaining E-BMP-2 (50 μg/side or more) had in a larger bending load than that from animals treated with autogenous bone grafts.

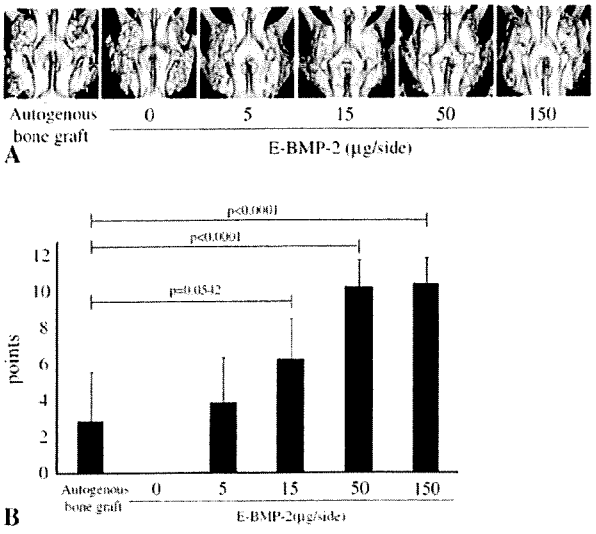

Fig. 1A–B (A) Representative 3D-CT images of posterolateral fusion at 8 weeks after surgery are shown. Fusion masses of groups of BMP15, BMP50 and BMP150 are well remodeled as is the autogenous bone graft group. E-BMP-2 treatment could radiographically achieve lumbar spinal fusion the same as autogenous bone graft. (B) Radiological fusion scores of 3D-CT of BMP50 and BMP150 were higher than autogenous bone graft control group. Values are mean ± standard deviation (SD).

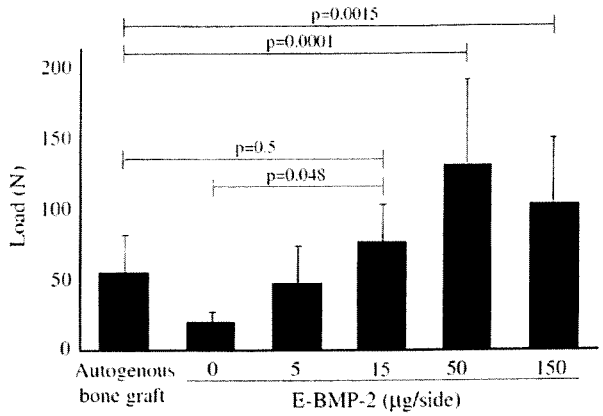

Fig. 2 The bending load at 1-mm middle-span deflection of the fusion mass of the BMP15 group was similar to that of autogenous bone graft control group. More than 15 μg/side of E-BMP-2 treatment could mechanically achieve lumbar spinal fusion as well as autogenous bone graft. The bending loads of the BMP50 and BMP150 were higher than that of the autogenous bone graft control group. Values are mean ± SD.

Histological examination revealed E-BMP-2 adsorbed β-TCP granules achieved fusion between transverse processes as well as autogenous bone graft. Eight weeks after operation, the bone masses with the peripheral cortical bone bridging the transverse processes achieved with more than 50 μg/side of E-BMP-2 (Fig. 3D, E, J and G) were similar to those achieved with autogenous bone graft (Fig. 3F and L) although the groups treated with less than 15 μg/side of E-BMP-2 (Fig. 3A–C, G–I) could not be achieved complete bone bridging. Toluidine blue-stained specimens from the groups of BMP5, BMP15, and the autogenous bone grafting control group (Fig. 4B and H, C and I, F and L, respectively) revealed metachromatic cartilage formation in the middle of the new bony mass bridging the transverse processes though there is no cartilage residue in the bone mass between transverse processes of the groups treated with more than 50 μg/side of E-BMP-2 (Fig. 4D and E). Higher-magnification views of bridging bone masses showed remaining β-TCP granules in these groups (Fig. 4G–K). In the controls without E-BMP-2, only fibrous tissue and remaining β-TCP without new bone were seen (Fig. 4A and G). The amount of β-TCP remaining within new bone mass was reduced ($p < 0.0001$) in all BMP groups compared with the control group treated without E-BMP-2 (Fig. 5). Furthermore, within newly formed bone in the E-BMP-2-treated groups (Fig. 6A–D), osteoclasts (TRAP-positive giant cells) were predominantly seen on the surfaces of the β-TCP in a dose dependent manner (Fig. 6E–H), suggesting more rapid resorption of β-TCP within the BMP-induced new bone mass and remodeling of the fusion masses.

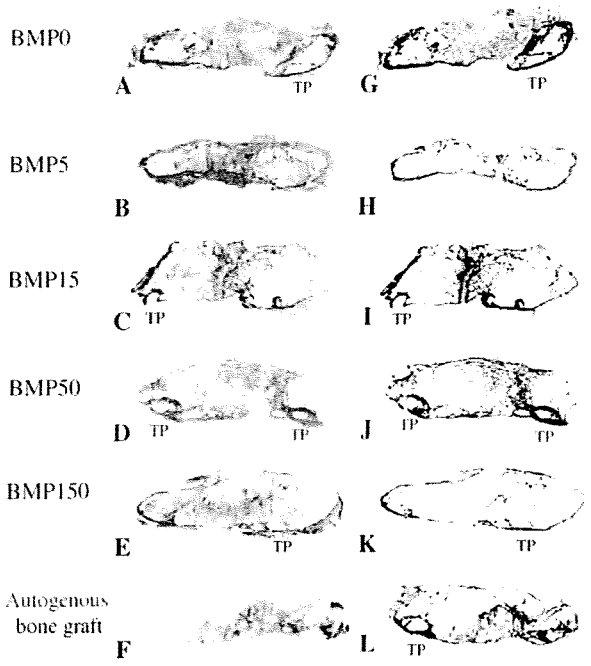

Fig. 3A–L Representative longitudinal histology sections of fusion mass of each group 8 weeks after surgery are shown. (**A**) BMP0; (**B**) BMP5; (**C**) BMP15; (**D**) BMP50; (**E**) BMP150; (**F**) autogenous bone graft (Stain, hematoxylin and eosin; original magnification, ×1). (**G**) BMP0; (**H**) BMP5; (**I**) BMP15; (**J**) BMP50; (**K**) BMP150; (**L**) autogenous bone graft (Stain, von Kossa and van Gieson; original magnification, ×1). Newly formed bone mass between transverse processes of BMP50 and 150 showed completely continuous cortical bone as well as autogenous bone graft control group. More than 50 μg/side of E-BMP-2 treatment could histologically achieve lumbar spinal fusion as well as autogenous bone graft.

Discussion

BMPs were originally identified as osteoinductive proteins by Urist more than 40 years ago. Since cloning of BMP genes, studies of BMPs and their clinical application have advanced. However, with progression of clinical application, issues related to drug delivery systems and production costs have arisen. β-TCP granules are widely used in clinical situations and E. coli-derived rhBMP-2 (E-BMP-2) can be produced at less cost compared with mammalian cell-derived BMP-2. Therefore we asked whether E. coli-derived rhBMP-2 (E-BMP-2) adsorbed on porous β-TCP granules could achieve posterolateral lumbar fusion in a rabbit model similar to that of autogenous bone graft.

We note several limitations. First, we used a rabbit posterolateral spinal fusion model. For clinical application, studies must be performed in much larger animals including sheep or nonhuman primates since the efficacy of cytokines and BMPs vary in differing species. Second, we followed the process of spinal fusion for only 8 weeks. Although this time period was determined by longitudinal

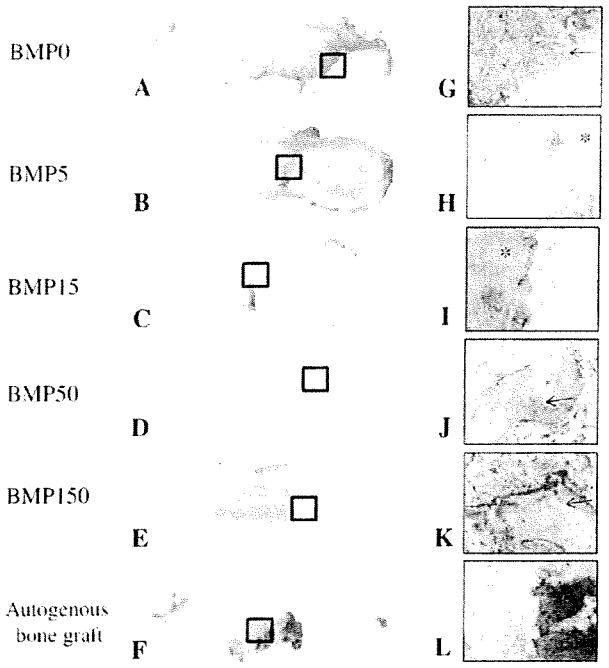

Fig. 4A–L Representative longitudinal histology sections of fusion mass of each group at 8 weeks after surgery are shown. (**A**) BMP0; (**B**) BMP5; (**C**) BMP15; (**D**) BMP50; (**E**) BMP150; (**F**) autogenous bone graft (Stain, Toluidine blue; original magnification, **A–F**: ×1). (**G**) BMP0; (**H**) BMP5; (**I**) BMP15; (**J**) BMP50; (**K**) BMP150; (**L**) autogenous bone graft (Metachromatic; original magnification ×100 for **G** and **L**, original magnification ×200 for **H**, **I**, **J** and **K**). Positive cartilage remnant in the fusion mass is not present in only section of groups of BMP50 and BMP150. More than 50 μg/side of E-BMP-2 treatment could histologically achieve lumbar spinal fusion as well as autogenous bone graft. Arrows indicate residual β-TCP.

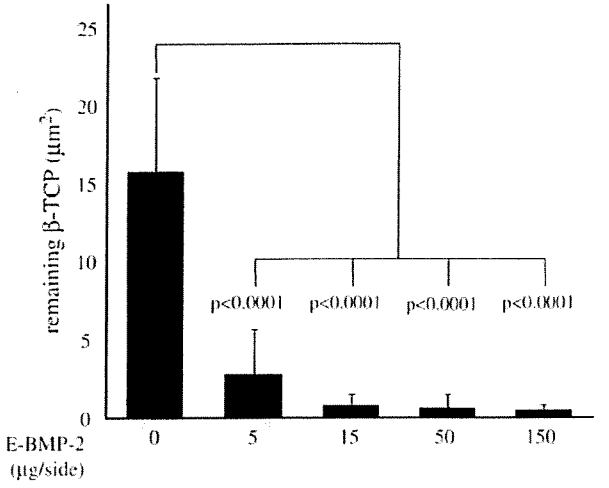

Fig. 5 Amounts of residual β-TCP were quantitatively assessed using bone histomorphometry software and expressed per square micron. Resorption of β-TCP was higher in the groups treated with E-BMP-2 than in the group treated without E-BMP-2. E-BMP-2 treatment could histologically achieve remodeling of newly formed fusion mass the same as autogenous bone graft. Values are mean ± SD.

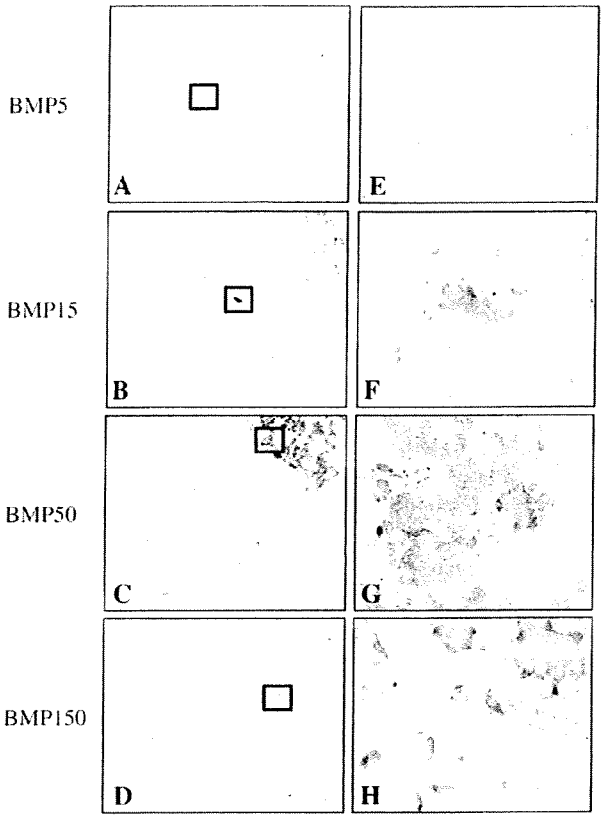

Fig. 6A–H Representative longitudinal histology sections of fusion mass of each group at 4 weeks after surgery are shown. (**A** and **E**) BMP5; (**B** and **F**) BMP15; (**C** and **G**) BMP50; (**D** and **H**) BMP150. (Stain, TRAP; original magnification, **A–D**: x100, **E–H**: ×400). Right panels show higher magnifications of each left panel. E-BMP-2 treatment could histologically achieve remodeling of newly formed fusion mass as same as autogenous bone graft. TRAP-positive giant cells, that are osteoclasts, are abundant in the BMP50 and BMP150 groups.

followup of 3D-CT, different results might have been obtained at later stages. Third, our sample size in each group was not sufficient to yield substantial effects and the study is likely underpowered; we therefore consider the study preliminary. On the other hand, we previously found E-BMP-2 has osteoinductive activity equivalent to that currently produced in BMP-2 gene-transfected animal cells (Chinese hamster ovary cells) [45]. However, it is essential to evaluate the safety of E-BMP-2 for clinical use. In several previous studies using E-BMP-2 [18, 29, 45], its safety was not sufficiently examined. Evaluation of the safety of E-BMP-2 is required in preclinical studies.

One problem with wide clinical use of BMPs is their high cost of production, since they are originally derived from mammalian CHO cells [42]. To address this issue, Sebald et al. devised a novel method to produce rhBMP-2 derived from E. coli and convert BMP monomers to biologically active dimers (E-BMP-2) [18, 29]. E-BMP-2 has